ISSN 1674-1056
http://cpb.iphy.ac.cn
http://iopscience.iop.org/cpb
中国物理 B
Chinese Physics
中国物理 Chinese Physics B

Enhancement of electron-ion recombination rates at low energy range in the heavy ion storage ring CSRm

Nadir Khan, Zhong-Kui Huang(黄忠魁), Wei-Qiang Wen(汶伟强), Shu-Xing Wang(汪书兴), Han-Bing Wang(汪寒冰), Wan-Lu Ma(马万路), Xiao-Long Zhu(朱小龙), Dong-Mei Zhao(赵冬梅), Li-Jun Mao(冒立军), Jie Li(李杰), Xiao-Ming Ma(马晓明), Mei-Tang Tang(汤梅堂), Da-Yu Yin(殷达钰), Wei-Qing Yang(杨维青), Jian-Cheng Yang(杨建成), You-Jin Yuan(原有进), Lin-Fan Zhu(朱林繁), Xin-Wen Ma(马新文)

Citation: Chin. Phys. B . 2020, 29(3): 033401 . **doi:** 10.1088/1674-1056/ab69eb
Journal homepage: http://cpb.iphy.ac.cn; http://iopscience.iop.org/cpb

What follows is a list of articles you may be interested in

Investigations of the dielectronic recombination of phosphorus-like tin at CSRm

Xin Xu(许鑫), Shu-Xing Wang(汪书兴), Zhong-Kui Huang(黄忠魁), Wei-Qiang Wen(汶伟强), Han-Bing Wang(汪寒冰), Tian-Heng Xu(徐天衡), Xiao-Ya Chuai(啜晓亚), Li-Jun Dou(豆丽君), Wei-Qing Xu(徐卫青), Chong-Yang Chen(陈重阳), Chuan-Ying Li(李传莹), Jian-Guo Wang(王建国), Ying-Long Shi(师应龙), Chen-Zhong Dong(董晨钟), Li-Jun Mao(冒立军), Da-Yu Yin(殷达钰), Jie Li(李杰), Xiao-Ming Ma(马晓明), Jian-Cheng Yang(杨建成), You-Jin Yuan(原有进), Xin-Wen Ma(马新文), Lin-Fan Zhu(朱林繁)

Chin. Phys. B . 2018, 27(6): 063402 . **doi:** 10.1088/1674-1056/27/6/063402

Positronium formation for positron scattering from metastable hydrogen

Lin Lin(林蔺), Hong-Nian Wang(汪宏年), Li-Guang Jiao(焦利光)

Chin. Phys. B . 2017, 26(3): 033401 . **doi:** 10.1088/1674-1056/26/3/033401

Theoretical study on photorecombination of C V ion

Ma Kun, Xie Lu-You, Zhang Deng-Hong, Dong Chen-Zhong

Chin. Phys. B . 2015, 24(7): 073402 . **doi:** 10.1088/1674-1056/24/7/073402

Fast-electron-impact ionization process by 3p of hydrogen-like ions in Debye plasmas

Qi Yue-Ying, Ye Dan-Dan, Wang Jian-Guo, Qu Yi-Zhi

Chin. Phys. B . 2015, 24(3): 033403 . **doi:** 10.1088/1674-1056/24/3/033403

Charge state effect on the K-shell ionization of iron by xenon ions near the Bohr velocity

Zhou Xian-Ming, Zhao Yong-Tao, Ren Jie-Ru, Cheng Rui, Lei Yu, Sun Yuan-Bo, Xu Ge, Wang Yu-Yu, Liu Shi-Dong, Xiao Guo-Qing

Chin. Phys. B . 2013, 22(11): 113402 . **doi:** 10.1088/1674-1056/22/11/113402

Enhancement of electron–ion recombination rates at low energy range in the heavy ion storage ring CSRm*

Nadir Khan[1,2], Zhong-Kui Huang(黄忠魁)[1], Wei-Qiang Wen(汶伟强)[1,2,†], Shu-Xing Wang(汪书兴)[3], Han-Bing Wang(汪寒冰)[1], Wan-Lu Ma(马万路)[3], Xiao-Long Zhu(朱小龙)[1,2], Dong-Mei Zhao(赵冬梅)[1], Li-Jun Mao(冒立军)[1,2], Jie Li(李杰)[1], Xiao-Ming Ma(马晓明)[1], Mei-Tang Tang(汤梅堂)[1], Da-Yu Yin(殷达钰)[1], Wei-Qing Yang(杨维青)[1], Jian-Cheng Yang(杨建成)[1,2], You-Jin Yuan(原有进)[1,2], Lin-Fan Zhu(朱林繁)[3], and Xin-Wen Ma(马新文)[1,2,‡]

[1] *Institute of Modern Physics, Chinese Academy of Sciences, Lanzhou* 730000, *China*
[2] *University of Chinese Academy of Sciences, Beijing* 100049, *China*
[3] *Hefei National Laboratory for Physical Sciences at Micro-scale, Department of Modern Physics, University of Science and Technology of China, Hefei* 230026, *China*

(Received 28 November 2019; revised manuscript received 6 January 2020; accepted manuscript online 10 January 2020)

Recombination of Ar^{14+}, Ar^{15+}, Ca^{16+}, and Ni^{19+} ions with electrons has been investigated at low energy range based on the merged-beam method at the main cooler storage ring CSRm in the Institute of Modern Physics, Lanzhou, China. For each ion, the absolute recombination rate coefficients have been measured with electron–ion collision energies from 0 meV to 1000 meV which include the radiative recombination (RR) and also dielectronic recombination (DR) processes. In order to interpret the measured results, RR cross sections were obtained from a modified version of the semi-classical Bethe and Salpeter formula for hydrogenic ions. DR cross sections were calculated by a relativistic configuration interaction method using the flexible atomic code (FAC) and AUTOSTRUCTURE code in this energy range. The calculated RR + DR rate coefficients show a good agreement with the measured value at the collision energy above 100 meV. However, large discrepancies have been found at low energy range especially below 10 meV, and the experimental results show a strong enhancement relative to the theoretical RR rate coefficients. For the electron–ion collision energy below 1 meV, it was found that the experimentally observed recombination rates are higher than the theoretically predicted and fitted rates by a factor of 1.5 to 3.9. The strong dependence of RR rate coefficient enhancement on the charge state of the ions has been found with the scaling rule of $q^{3.0}$, reproducing the low-energy recombination enhancement effects found in other previous experiments.

Keywords: storage ring, electron cooler, highly charged ions, radiative recombination enhancement

PACS: 34.80.Lx, 29.20.db, 32.30.–r **DOI:** 10.1088/1674-1056/ab69eb

1. Introduction

Electron–ion recombination is one of the most fundamental atomic collision processes, and plays an important role in plasma physics, astrophysics as well as accelerator physics.[1] The experimentally obtained electron–ion recombination rate coefficients can be not only used to study the energy level structure of highly charged ions, thereby testing the theoretical methods for atomic structures calculation, but also used as the basic input parameters for plasma diagnosis and modeling to interpret the emission spectrum of astrophysical and man-made plasmas.[2] Additionally, the electron–ion recombination also reduces the lifetime of the ion beam which leads to the positive ions loss mechanism during electron cooling, particularly at high ion charge state and high beam velocity when the residual gas processes become less important.[3] The electron–ion recombination with its large cross section and rates at the low energies also provides a very favorable scheme for the production of antihydrogen.[4] However, most of these electron–ion recombination cross sections are calculated by different theories with limited accuracy, and experimental studies to benchmark these theories are very important and have been already investigated for decades. There are two most dominating electron–ion recombination channels for low energy collision range called radiative recombination (RR) and dielectronic recombination (DR). The RR is a one-step non-resonant process where a free electron recombines with an ion by simultaneously emitting a photon to release the excess energy

$$A^{q+} + e(E) \rightarrow A^{(q-1)}(n) + h\nu. \tag{1}$$

The DR is a two-step resonant recombination process, where a free electron recombines with the ion resonantly exciting another core electron. In the second step the system stabilizes itself by emitting a photon. This process can be interpreted as

*Project supported by the National Key Research and Development Program of China (Grant No. 2017YFA0402300) and the National Natural Science Foundation of China (Grant Nos. U1932207, 11904371, and U1732133).

†Corresponding author. E-mail: wenweiqiang@impcas.ac.cn
‡Corresponding author. E-mail: x.ma@impcas.ac.cn

© 2020 Chinese Physical Society and IOP Publishing Ltd

a time reversed Auger emission

$$A^{q+} + e(E) \rightarrow A^{(q-1)+**} \rightarrow A^{(q-1)+*}(n) + h\nu. \quad (2)$$

Heavy-ion storage rings equipped with electron coolers are powerful tools for experimental study of the electron–ion collision processes at the well-controlled relative energy. A very low collision energies down to few meV can be only achieved and investigated by using electron and ion beams of nearly same velocities by the merged-beams technique at storage rings.[5] In these experiments, the ion beam is merged with a cold and magnetically guided electron beam in the electron cooler where the electron beam offers not only the cooling medium for the ion beam but also is used as a cold electron target for electron–ion recombination.

The first radiative recombination experiment at low energy was performed by merging C^{6+} ion beam with an electron beam in a single pass arrangement by Andersen *et al.*[6] In that experiment a good agreement has been found between measured recombination rates and calculated results in the energy range from $E_{\rm rel} = 0$ eV to 1 eV, where $E_{\rm rel}$ is the relative collision energy between electrons and ions. However, a significant enhancement effect beyond the theoretical calculation has been found in a range of low relative energies between electron and ions in the RR experiments. In order to understand this rate enhancement phenomenon, a series of electron–ion recombination experiments with many bare ions (D^+, He^{2+}, C^{6+}, N^{7+}, Ne^{10+}, Si^{14+}, Ar^{18+}, Bi^{83+}) have been performed to investigate this RR enhancement effect at different storage rings.[5,7–13] These works test the variation of electron beam density,[14] the influence of magnetic field,[5] and also the dependence of charge state.[9] Strong enhancement effects have been observed for all of these measured RR rate coefficients as compared with the theoretical rate coefficients at a very low electron–ion collision energies ($E_{\rm rel} < 10$ meV).

In addition to the bare-ions, the RR rate enhancement has also been observed in experiments with non-bare ions at the storage rings.[15–19] However, because of the complex electronic structure of non-bare ions, neither a concentrated study is available for these enhanced rates, nor have detailed quantitative spectra in low relative energy region have been presented. To explain this surprising discrepancy between the measured RR recombination rate coefficients and the theoretical predictions, several theoretical models and mechanisms have been proposed ranging from the contributions from three body recombination (TBR),[9] the electron density enhancement in the surrounding of the ions due to plasma screening effect[20] and the effect of magnetic field taking into account the chaotic dynamic as a result of the magnetic field inside the electron cooler which directly influence the cross sections.[21] Some of the models also included the contribution of transient field effects by a magnetic field in the electron-cooler[22] and relativistic effects by using Dirac–Slater method together with multichannel quantum defect theory (MQDT).[23,24] Finally, one model by taking into account of the transient field effects from a magnetic field explained the observed RR enhancement phenomenon with only bare ions.[25]

An approach presented in this work is mainly focused on the investigation of RR rate enhancement in electron–ion recombination spectra for non-bare highly charged ions. Recombination of Ar^{14+}, Ar^{15+}, Ca^{16+}, and Ni^{19+} ions with electrons at low energy range have been investigated based on the merged-beam method at the main cooler storage ring CSRm. In order to interpret the measured results, RR cross sections were obtained from a modified version of the semi-classical Bethe and Salpeter formula for hydrogenic ions. DR cross sections were calculated by a relativistic configuration interaction method using the flexible atomic code (FAC) and AUTOSTRUCTURE code in this energy range. The calculated total rate coefficients show a good agreement with the measured rate coefficients above 100 meV. However, large discrepancies have been found at the low energy range especially below 10 meV. As the relative collision energy decreases below 1 meV, it is found that the observed recombination rates are a factor of 1.5 to 3.9 higher than the predicted rates. The dependence of RR rate coefficient enhancement as a function of the charge state of the ions has been obtained and compared with bare ions.

The article is arranged as follow. In Section 2 we will discuss the experimental set up and methods regarding to the merged beams electron–ion recombination at the CSRm with some important parameters. Section 3 will briefly describe the theoretical approach related to RR and DR, with the modified semi-classical Bethe and Salpeter formula for RR and the AUTOSTRUCTURE and FAC codes implementation for DR. Section 4 presents the experimental results and comparison with the current calculations. Additionally, the experimental data are scaled as a function of the nuclear charge state of the ions and also compared with different results from literature. Section 5 is concerning with the conclusion of the present work.

2. Experimental method

The measurement of electron–ion recombination with highly charged ions has been performed by employing the merged beams method at the CSRm at Institute of Modern Physics (IMP) in Lanzhou, China (See Fig. 1). The main features of the experimental technique were described in the previous papers and Refs. [26–28]. Here we will just briefly describe the general experimental method and important parameters related to the present work. The highly charged ions were produced in the ECR ion sources,[29] and then supplied by a

sector focused cyclotron (SFC) to the CSRm after acceleration. One injection pulse of ions from the SFC into CSRm was enough to provide the typical ion current of 50 μA–150 μA which corresponds to the number of ions 1×10^8–3×10^8. The ion beam lifetime is around 50 s. The ion-beam was merged with the magnetically confined electron-beam of the cooler in one straight section with typical length of 4.0 m of the CSRm storage ring.

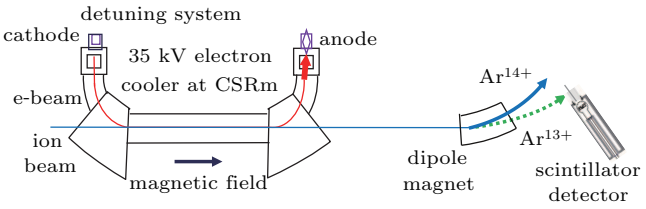


Fig. 1. The schematic view of the electron cooler and the experimental setup for electron–ion recombination experiment at the CSRm, Lanzhou. The electron beam produced at the cathode is guided by magnetic field, then merges with ion beam at the straight section of 4.0 m. The electron-beam is then separated from the ion-beam by the magnetic guiding field and collected by the anode. In a dipole magnet downstream to the electron cooler the recombined ions are separated from the primary ion beam, and then counted by a scintillator detector.

The ion beams have been cooled for several seconds by employing electron cooler (EC-35) before starting a measurement until the beam profile reached to their equilibrium spread. The electron-beam was confined at the cathode section of the electron cooler with magnetic field of 125 mT and adiabatically expanded at the cooler section with 39 mT, respectively. This expansion gives rise to cold electron beam for high resolution spectroscopy. The magnetically confined electron beam at the cooler section has a radius of ~ 25 mm, with a typical electron density of 1×10^6 cm^{-3}. Besides electron cooling, the electron cooler is also used as an electron target during the electron–ion recombination measurement. For a change of the electrons energy from cooling energy, the detuning system has been applied to the cathode of the electron cooler. For introducing non-zero mean relative velocities between the electrons and ions, the electron energy was stepped through a preset range of values different from the cooling energy during the measurement cycle. The measurement cycle includes different detuning voltages of 1 V in laboratory system. In each measurement interval, the electron energy was detuned for 10 ms and again set to the cooling energy ($E_{\rm rel}=0$) for 90 ms or 190 ms in order to maintain a good ion-beam quality. The recombined ions formed in the merging section were separated by the first dipole magnet downstream the electron cooler and detected by a scintillator detector.[30]

At storage rings, the recombination rate coefficients α measured at scanning energy $E_{\rm rel}$, between electron and ion is determined by

$$\alpha(E_{\rm rel})=\frac{R}{N_{\rm i}n_{\rm e}(1-\beta_{\rm e}\beta_{\rm i})}\cdot\frac{C}{L} \tag{3}$$

with R denoting the electron–ion recombination count rate, $N_{\rm i}$ is the number of stored ions, $n_{\rm e}$ is the density of electron beam, $L=4.0$ m is the length of the effective interaction section and $C=161$ m is the circumference of storage ring. $\beta_{\rm e}$ and $\beta_{\rm i}$ correspond to the velocities of electron and ion beams respectively. The estimated systematic uncertainty in CSRm experiment is 30%. The experimental rate coefficient is related to the cross section as

$$\alpha(E)=\langle\upsilon\sigma\rangle=\int_{-\infty}^{+\infty}\upsilon\sigma(\upsilon)f(\upsilon,T_{\parallel},T_{\perp})\,{\rm d}^3\upsilon, \tag{4}$$

where $f(\upsilon,T_{\parallel},T_{\perp})$ is a flattened Maxwellian distribution that is characterized by the longitudinal and transverse temperatures of the electron beam[31]

$$f(\upsilon,T_{\parallel},T_{\perp})=\sqrt{\frac{m_{\rm e}}{2\pi k_{\rm B}T_{\parallel}}}\exp\left[-\frac{m_{\rm e}(\upsilon_{\parallel}-\upsilon)^2}{2k_{\rm B}T_{\parallel}}\right]\times\frac{m_{\rm e}}{2\pi k_{\rm B}T_{\perp}}\exp\left(-\frac{m_{\rm e}\upsilon_{\perp}^2}{2k_{\rm B}T_{\perp}}\right). \tag{5}$$

In Eq. (5), $T_{\perp}$ and $T_{\parallel}$ are the transverse and longitudinal temperatures to the motion of the electron beam direction respectively. $k_{\rm B}$ is the Boltzmann constant, $m_{\rm e}$ is the mass of electron. The theoretical approach for possible explanation of the experimental results is given below.

3. Theoretical approach

The calculation of the RR cross section is based on the modified semi-classical formula of Bethe & Salpeter in this work. RR of high-Z bare ions with cold electrons can be treated within the non-relativistic dipole approximation. Bethe and Salpeter derived a simple formula for RR cross section calculation,[32]

$$\sigma^{\rm RR}(n,E_{\rm rel})=(2.105\times10^{-22}\ {\rm cm}^2)\frac{E_0^2}{nE_{\rm rel}(E_0+n^2E_{\rm rel})}. \tag{6}$$

In this case the $E_0=q^2R$ is the binding energy of the ground state electron in H-like ions with charge q and Rydberg constant $R=13.6$ eV, $E_{\rm rel}$ is the kinetic energy in electron–ion center-of-mass frame, the electron capture by a bare ion produces a hydrogenic state with principal quantum number n. The total cross section is then given as

$$\sigma^{\rm RR}(E)=\sum_{n=1}^{n_{\rm max}}\sigma^{\rm RR}(n,E), \tag{7}$$

where $n_{\rm max}$ is the maximum principal quantum number, related to the ionization limit of the dipole magnet in experimental setup. The classical expression given in Eq. (6) is only valid for high quantum number $n\gg1$, and in limit of low electron energies $E_{\rm rel}=Z^2/n^2R_y$. The classical approach was corrected by introducing the correction factor $G_n(E_{\rm rel})$, which are usually weakly dependent on energy. This factor is known as Gaunt factor in literature and provides the correction for the

deviation of Bethe & Salpeter classical approach from quantum mechanical approach for low n RR. Thus, the RR cross section for hydrogenic ions into a bound nl state is given by

$$\sigma^{\mathrm{RR}}(E) = 2.105\times10^{-22}\ \mathrm{cm}^2 \times \sum_{n_{\min}}^{n_{\max}} k_n t_n \frac{q^2R^2}{nE(q^2R+n^2E)}, \quad (8)$$

where the value of the principal quantum number $n_{\max}$ was determined by field ionization in the dipole magnet, for different ions the $n_{\min}$ and $n_{\max}$ values should be different as for Ni^{19+} the summation was carried out from $n_{\min}=2$ to $n_{\max}=96$. The R is the Rydberg constant, q is the effective charge, the constant t_n accounts for partly filled shells, the $k_n = G_n(0)$ is the Gaunt-factor. The value of Gaunt factor in this work was calculated by following the prescription of Anderson & Balko (1990). The calculated RR cross section later is convoluted by the experimental electron velocity distribution (see Eqs. (4) and (5)). After convolution, the RR rate coefficient was modified with a factor which was obtained from the fitting of the experimental data. This modification of the calculated RR rate coefficient by a factor to achieve the matching, indicate that using of hydrogenic approximation for non-bare multi-electron system is not appropriate.

In the present experiments all of the ions which have been measured are non-bare and the contribution from DR resonance process could not be avoided. Therefore, the DR process must be considered in the theoretical calculations for better investigation of the electron–ion recombination spectra at very low energy range. The theoretical calculations of DR for Be-like Ar^{14+} and Be-like Ca^{16+} have been performed by using distorted-wave collision package AUTOSTRUCTURE.[33] For the Li-like Ar^{15+} and F-like Ni^{19+} the FAC[34] was used to calculate DR resonance cross sections. It should be noted that the difference between these two codes are described in Ref. [35] The integrated DR cross section for state d can be written as

$$\hat{\sigma}_d = a_0^2 \frac{g_d}{2g_i}\frac{2\pi^2\hbar R}{E_d}\frac{A_a(d\to i)\sum_f A_r(d\to f)}{\sum_k A_a(d\to k)+\sum_{f'}A_r(d\to f')}, \quad (9)$$

where g_i and g_d are the statistical weights for the initial and intermediate states, R is the Rydberg state, a_0 is the Bohr radius,E_d is the resonance energy, i, d, and f denote the initial, intermediate, and final states respectively. A^r and A^a are the radiative and autoionization rates respectively. The k denotes all the possible states by autoionization of the intermediate states. The total cross section for DR is given by

$$\sigma(E) = \sum_d \sigma_d(E). \quad (10)$$

The details about the DR calculation method for Be-like Ar^{14+}, Be-like Ca^{16+}, and F-like Ni^{19+}can be found in Refs. [2,36,37]. Instead of separate calculations of RR and DR contributions, the total recombination rate coefficient can be derived by adding the continuous RR background to the DR spectrum including the AUTOSTRUCTURE and FAC calculations.

4. Results and discussion

Figure 2 shows the absolute recombination rate coefficient for Be-like Ar^{14+}, Li-like Ar^{15+}, Be-like Ca^{16+}, and F-like Ni^{19+} ions as functions of electron–ion collision energies. The electron–ion recombination spectra include RR and DR and cover the energy range of 0 meV–1000 meV in the center of mass energy frame. In Fig. 2(a), the total experimental recombination rate coefficient is represented by connected black solid circles, dashed violet lines denote theoretical RR rate coefficient. The green solid lines denote the sum of calculated RR and DR rate coefficients, which was obtained from the convolution of calculated RR and DR cross section with the anisotropic electron velocity distribution. However, a very large discrepancy can be found between the experimental results and the theoretical calculations, because the theoretical results of DR rate coefficients have very large uncertainties for multi-electron ions in low energy range. For accurate determination of the electron beam temperature in each experiment, we fitted each spectrum with several DR resonance line profile. In the fit for each line profile the corresponding cross sections were convoluted with the same function as shown in Eq. (5), which can be rewrite as

$$\alpha_d(\upsilon_{\mathrm{rel}}) = \frac{\hat{\sigma}_d\upsilon_d}{m_e\sigma_\perp^2\zeta}\exp\left(-\frac{\upsilon_d^2-\upsilon_{\mathrm{rel}}^2\zeta^{-2}}{\sigma_\perp^2}\right) \times\left[\mathrm{erf}\left(\frac{\upsilon_{\mathrm{rel}}+\upsilon_d\zeta^2}{\sigma_\parallel\zeta}\right)-\mathrm{erf}\left(\frac{\upsilon_{\mathrm{rel}}-\upsilon_d\zeta^2}{\sigma_\parallel\zeta}\right)\right], \quad (11)$$

where $\hat{\sigma}_d\upsilon_d = \int\alpha_d(\upsilon_0(E_0))\mathrm{d}E_0$, υ_d represents the relative velocity related to the resonance energy E_d, ζ is given as $\zeta=\sqrt{1-T_\parallel/T_\perp}$, and $\sigma_{\parallel,\perp}$ is $\sigma_{\parallel,\perp}=\sqrt{2kT_{\parallel,\perp}/m_e}$.

Therefore, from the fitting of the line profile given by Eq. (11) to the measured resonance profile, the transverse and longitudinal temperatures of the electron beam can be obtained,[31] as shown in Fig. 2(b). The solid red line is the fitted results including RR + DR. It should be noted that the first resonance peak was treated as a Lorentzian line shape multiplied by a factor of E_{res}/E in each fitting.[18] The obtained transverse and longitudinal temperatures of electron beam were $k_BT_\parallel = 0.56(7)$ meV and $k_BT_\perp = 23(1)$ meV for the Ni^{19+}, $k_BT_\parallel = 2.40(6)$ meV and $k_BT_\perp = 11.91(87)$ meV for Ar^{14+}, $k_BT_\parallel = 0.8$ meV and $k_BT_\perp = 40$ meV for Ar^{15+} and Ca^{16+}, respectively. It can be found that the experimental RR rate coefficient exceeds the fitting and theoretical results a_0 at low electron–ion collision energy below 10 meV as shown in Fig. 2(b). This effect is known as the RR rate

coefficient enhancement, which can be written as $\Delta\alpha$, where $\Delta\alpha = \alpha_{\text{Experiment}} - \alpha_0$ is the difference between experimental result $\alpha_{\text{Experiment}}$ and fitting result α_0. The RR enhancement factor can be defined as $\varepsilon - 1 = \Delta\alpha/\alpha_0$. At energies below 4 meV, the experimental rate coefficient shows an enhancement ($\Delta\alpha$) over a fitted rate coefficient (α_0) by a factor of about 3.9 for Ar^{15+}, 1.9 for Ar^{14+}, 1.5 for Ca^{16+}, and 2.1 for Ni^{19+}, respectively.

From the theoretical model described in,[38] the relationship between the recombination rate coefficient enhancement $\Delta\alpha^{\text{RR}}$ to the main physical parameters concerning to electron–ion recombination experiments can be written as

$$\Delta\alpha^{\text{RR}} \propto Z^{2+\mu} B^{\mu} T_{\perp}^{-(3\mu+\nu+1)2} T_{\parallel}^{\nu/2}. \tag{12}$$

This is known as the scaling law for recombination in electron cooler.[5] Here Z is the charge state of the ion, B is the guiding magnetic field in the electron cooler, $T_{\perp}$ and $T_{\parallel}$ are the transverse and longitudinal temperatures, μ and ν are the fitting parameters.[39] In order to compare our results with RR enhancement effects observed from bare ions, the scaling law has been fitted for the nuclear charge state of the bare ions in other storage rings measurements and non-bare ions from the present investigation as show in Figs. 3(a) and 3(b), respectively.

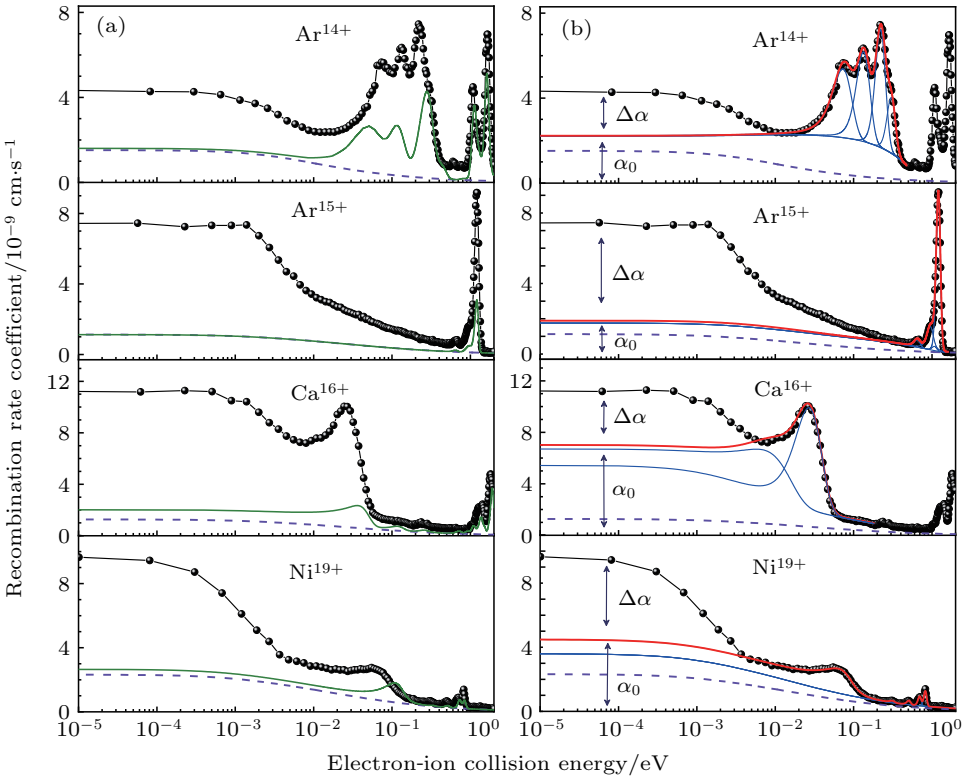


Fig. 2. The absolute recombination rate coefficient for Be-like Ar^{14+}, Li-like Ar^{15+}, Be-like Ca^{16+}, and F-like Ni^{19+} respectively. (a) Comparison of the experimental result to the theoretical calculations, the experimental data represented by connected black solid circles, the violet dashed line is for RR rate coefficient and the green line is from theoretical data of RR + DR. (b) Comparison of the experimental results with fitted data by taking into account of RR + DR resonances. Blue solid line corresponds to the fitting of DR. The red solid line indicates the fitted data including RR + DR, and $\Delta\alpha$ is the enhancement of the experimental rate coefficient over the fitted rate coefficient α_0. The transverse and longitudinal temperature obtained from this fitting are $k_B T_{\parallel} = 2.40(6)$ meV and $k_B T_{\perp} = 11.91(87)$ meV for Ar^{14+} and $k_B T_{\parallel} = 0.8$ meV, $k_B T_{\perp} = 40$ meV for Ar^{15+} and Ca^{16+}, and $k_B T_{\parallel} = 0.56(7)$ meV and $k_B T_{\perp} = 23(1)$ meV for Ni^{19+}.

In Fig. 3(a), the RR enhancement factors from CRYRING[9] and TSR are shown[5] for the bare ions. Experimental uncertainty of 20% was estimated for all the bare ions data. The red solid line is the $q^{2.8}$ scaling, which is in agreement with the scaling behavior found at the CRYRING by Gao *et al.* (1997).[9] Figure 3(b) shows the excess RR rate coefficient $\Delta\alpha^{\text{RR}}$ for non-bare ions plotted as a function of nuclear charge state of the ions q by using scaling law. The empty green circles represent the present CSRm data for non-bare ions with 30% experimental uncertainty. The scaling of $q^{3.0}$ has been found for the excess rates for non-bare ions CSRm data as represented with the solid red line. It should be noted that the scaling law fitted very well to the bare ions data compared with non-bare ions.

In Fig. 3(b) the data for Li-like Ar^{15+} is away from the fitted line significantly. It might be due to the strong contribution from low laying DR resonances to the RR rate coefficient. These low laying DR resonances overlap with the RR rate coefficient near to threshold which results in the rate enhancement. For all other non-bare ions, the fitting is satisfactory which shows the validity of the scaling law for recombination experiments for both bare and non-bare ions at the storage

rings. These findings indicate that the low-energy DR resonances will overlap with the RR rate enhancement at very low electron–ion collision. One has to be careful when comparing the results from different facilities since the experimental conditions vary drastically. The influence from other parameters such as the transverse temperature $kT_{\perp}$, longitudinal temperature $kT_{\parallel}$, and magnetic field B has to be considered. Also one has to take into account of this RR rate enhancement and carefully subtract it from DR spectra during the investigation of the atomic structure by DR method. In addition, to the atomic structure studies, we also use this atomic data for x-ray astrophysical implications, the atomic databases such as AtomDB version 2.0 and XSPEC are used for modeling astrophysical plasmas. For these atomic databases one needs to transform the DR rate coefficients to the plasma rate coefficient, by convoluting it with average Maxwellian distribution. Since, from this work we conclude that the RR rate enhancement is concerning to the storage ring merged beams recombination method and we do not expect the RR enhancement effect in astrophysical environment. Therefore, one should subtract very carefully the RR enhancement from DR rate coefficient before transforming it to plasma rate coefficient. If the RR enhancement effect is not carefully subtracted from the DR spectra then the overlap between RR rate enhancement and DR resonances close to the threshold will be translated into plasma rate coefficient after convolution, which will create large uncertainties in theoretical and experimental data at the low energy range.

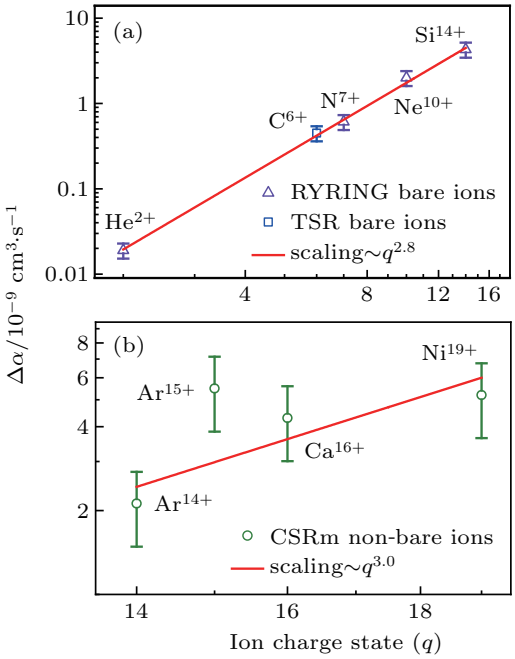


Fig. 3. (a) The dependence of the RR rate coefficient enhancement $\Delta\alpha$ of bare-ions on charge state of ions. The violet empty triangles represents experimental data of the CRYRING[8,9] and the blue color empty square is the TSR data.[5] The error bars represent the contribution from the uncertainty of the excess rate, in this plot 20% uncertainty has been assumed for all the data. The solid line is the $q^{2.8}$ scaling for the bare ions. (b) The dependence of the RR rate coefficient enhancement $\Delta\alpha$ of non-bare ions on the charge state q of the ions. The empty green circles represent experimental RR rate enhancement data of the CSRm for non-bare ions. The 30% experimental uncertainty has been taken and the solid red line is the $q^{3.0}$ scaling.

5. Conclusion

In this work, a series of measurement of the absolute recombination rate coefficients of Be-like Ar^{14+}, Li-like Ar^{15+}, Be-like Ca^{16+}, and F-like Ni^{19+} have been performed at the storage ring CSRm at Institute of Modern Physics, Lanzhou, China. Data analysis is focused on the electron–ion collision energy range from 0 meV to1000 meV. The experimental electron–ion recombination spectra have been fitted with flattened Maxwellian function which include the contributions from RR and DR processes. The theoretical results for RR rate coefficients were calculated by using modified semi-classical formula given by Bethe and Salpeter (1957). The contribution from DR rate coefficients to the recombination spectra were calculated by employing AUTOSTRUCTUTRE and FAC codes. A strong enhancement of the measured RR rate coefficient over the fitted and calculated rate coefficients have been observed in all recombination spectra for the collision energies below 10 meV.

The present evaluation of the nuclear charge dependence of the RR rate enhancement $\Delta\alpha$ results in $\sim Z^{3.0}$ scaling for non-bare ions. We have also compared our results with the RR enhancement factors from other storage rings for bare ions. Our recent findings indicate that the RR rate enhancement is a general phenomenon found in all storage ring measurements for both bare and non-bare ions. A smooth dependence of RR rate coefficient enhancement on nuclear charge states has been found for bare-ions. For the non-bare ions the RR rate enhancement dependence on nuclear charge is not smooth, which indicates that the enhancement is partly coming from the low-n DR resonances located close to the threshold. In addition, we have also pointed out that the RR enhancement rate strongly influences the DR resonances at very low relative energies which will also be translated to the plasma rate coefficient used for astrophysical implications.

Acknowledgement

The authors would like to thank the crew of the Accelerator Department for their skillful operation of the CSR accelerator complex. We would like to thank Chong-Yang Chen, Simon Preval and Nigel Badnell for theoretical calculations of DR spectra. One of the authors (Wen Wei-Qiang) thanks the support by the Youth Innovation Promotion Association of the Chinese Academy of Sciences.

References

[1] Müller A 2008 *Adv. Atom. Mol. Opt. Phys.* **55** 293

[2] Wang S X, Huang Z K, Wen W Q, Chen C Y, Schippers S, Xu X, Sardar S, Khan N, Wang H B, Dou L J, Mahmood S, Zhao D M, Zhu X L, Mao L J, Ma X M, Li J, Tang M T, Mao R S, Yin D Y, Yuan Y J, Yang J C, Shi Y L, Dong C Z, Ma X W and Zhu L F 2019 *Astron. Astrophys.* **627** A171

[3] Wolf A, Gwinner G, Linkemann J, Saghiri A A, Schmitt M, Schwalm D, Grieser M, Beutelspacher M, Bartsch T, Brandau C, Hoffknecht A, Müller A, Schippers S, Uwira O and Savin D W 2000 *Nucl. Instrum. Methods Phys. Res. Sect. A* **441** 183

[4] Holzscheiter M and Charlton M 1999 *Rep. Prog. Phys.* **62** 1

[5] Gwinner G, Hoffknecht A, Bartsch T, Beutelspacher M, Eklöw N, Glans P, Grieser M, Krohn S, Lindroth E, Müller A, Saghiri A A, Schippers S, Schramm U, Schwalm D, Tokman M, Wissler G and Wolf A 2000 *Phys. Rev. Lett.* **84** 4822

[6] Andersen L H, Bolko J and Kvistgaard P 1990 *Phys. Rev. Lett.* **64** 729

[7] Wolf A, Berger J, Bock M, Habs D, Hochadel B, Kilgus G, Neureither G, Schramm U, Schwalm D, Szmola E, Müller A, Wagner M and Schuch R 1991 *Z. Phys. D: Atoms. Molecules, Clusters* **21** S69

[8] Gao H, DeWitt D R, Schuch R, Zong W, Asp S and Pajek M 1995 *Phys. Rev. Lett.* **75** 4381

[9] Gao H, Schuch R, Zong W, Justiniano E, DeWitt D R, Lebius H and Spies W 1997 *J. Phys. B: At. Mol. Opt. Phys.* **30** L499

[10] Shi W, Böhm S, Böhme C, Hoffknecht A, Kieslich S, Schippers S, Müller A, Kozhuharov C and Bosch F 2001 *Eur. Phys. J. D* **15** 145

[11] Hoffknecht A, Schippers S, Muller A, Gwinner G, Schwalm D and Wolf A 2001 *Phys. Scr.* **2001** 402

[12] Hoffknecht A, Brandau C, Bartsch T, Böhme C, Knopp H, Schippers S, Müller A, Kozhuharov C, Beckert K, Bosch F, Franzke B, Krämer A, Mokler P H, Nolden F, Steck M, Stöhlker T and Stachura Z 2000 *Phys. Rev. A* **63** 012702

[13] Banaś D, Pajek M, Surzhykov A, Stöhlker T, Brandau C, Gumberidze A, Kozhuharov C, Beyer H, Böhm S and Bosch F 2015 *Phys. Rev. A* **92** 032710

[14] Gao H, Asp S, Biedermann C, DeWitt D R, Schuch R, Zong W and Danared H 1996 *Hyperfine Interact.* **99** 301

[15] Hoffknecht A, Bartsch T, Schippers S, Müller A, Eklöw N, Glans P, Beutelspacher M, Grieser M, Gwinner G and Saghiri A 1999 *Phys. Scr.* **1999** 298

[16] Schippers S, Müller A, Gwinner G, Linkemann J, Saghiri A A and Wolf A 2001 *Astrophys. J.* **555** 1027

[17] Shi W, Bartsch T, Böhme C, Brandau C, Hoffknecht A, Knopp H, Schippers S, Müller A, Kozhuharov C, Beckert K, Bosch F, Franzke B, Mokler P H, Nolden F, Steck M, Stöhlker T and Stachura Z 2002 *Phys. Rev. A* **66** 022718

[18] Schippers S, Schnell M, Brandau C, Kieslich S, Müller A and Wolf A 2004 *Astron. & Astrophys.* **421** 1185

[19] Schmidt E W, Schippers S, Müller A, Lestinsky M, Sprenger F, Grieser M, Repnow R, Wolf A, Brandau C, Lukić D, Schnell M and Savin D W 2006 *Astrophys. J.* **641** L157

[20] Spreiter Q and Toepffer C 2000 *J. Phys. B: At. Mol. Opt. Phys.* **33** 2347

[21] Hörndl M, Yoshida S, Tökési K and Burgdörfer J 2003 *Hyperfine Interact.* **146–147** 13

[22] Hörndl M, Yoshida S, Wolf A, Gwinner G and Burgdörfer J 2005 *Phys. Rev. Lett.* **95** 243201

[23] Wu Y, Zeng S L, Duan B, Yan J, Wang J G, Dong C Z and Ma X W 2007 *Chin. Phys. Lett.* **24** 404

[24] Zeng S L, Peng J Q, Li P, Li Y M, Yan J and Wang J G 2005 *Acta Phys. Sin.* **54** 2625 (in Chinese)

[25] Hörndl M, Yoshida S, Wolf A, Gwinner G, Seliger M and Burgdörfer J 2006 *Phys. Rev. A* **74** 052712

[26] Huang Z, Wen W, Wang H, Xu X, Zhu L, Chuai X, Yuan Y, Zhu X, Han X and Mao L 2015 *Phys. Scr.* **2015** 014023

[27] Xu X, Wang S X, Huang Z K, Wen W Q, Wang H B, Xu T H, Chuai X Y, Dou L J, Xu W Q and Chen C Y 2018 *Chin. Phys. B* **27** 063402

[28] Khan N, Huang Z K, Wen W Q, Mahmood S, Dou L J, Wang S X, Xu X, Wang H B, Chen C Y and Chuai X Y 2018 *Chin. Phys. C* **42** 064001

[29] Zhao H W, Sun L T, Guo J W, Lu W, Xie D Z, Hitz D, Zhang X Z and Yang Y 2017 *Phys. Rev. Accel. Beams* **20** 094801

[30] Wen W Q, Ma X, Xu W Q, Meng L J, Zhu X L, Gao Y, Wang S L, Zhang P J, Zhao D M, Liu H P, Zhu L F, Yang X D, Li J, Ma X M, Yan T L, Yang J C, Yuan Y J, Xia J W, Xu H S and Xiao G Q 2013 *Nucl. Instrum. & Methods Phys. Res. Sect. B* **317** 731

[31] Kilgus G, Habs D, Schwalm D, Wolf A, Badnell N R and Müller A 1992 *Phys. Rev. A* **46** 5730

[32] Bethe H A and Salpeter E E 2012 *Quantum mechanics of one-and two-electron atoms* (Springer Science & Business Media)

[33] Badnell N 2011 *Comput. Phys. Commun.* **182** 1528

[34] Gu M 2003 *Astrophys. J.* **590** 1131

[35] Savin D W, Kahn S M, Gwinner G, Grieser M, Repnow R, Saathoff G, Schwalm D, Wolf A, Muller A, Schippers S, Zavodszky P A, Chen M H, Gorczyca T W, Zatsarinny O and Gu M F 2003 *Astrophys. J. Suppl. Ser.* **147** 421

[36] Huang Z, Wen W, Xu X, Mahmood S, Wang S, Wang H, Dou L, Khan N, Badnell N and Preval S 2018 *Astrophys. J. Suppl. Ser.* **235** 2

[37] Wang S, Xu X, Huang Z, Wen W, Wang H, Khan N, Preval S, Badnell N, Schippers S and Mahmood S 2018 *Astrophys. J.* **862** 134

[38] Heerlein C, Zwicknagel G and Toepffer C 2002 *Phys. Rev. Lett.* **89** 083202

[39] Heerlein C, Zwicknagel G and Toepffer C 2003 *Nucl. Instrum. Methods Phys. Res. Sect. B* **205** 395